

Inactivation kinetics and lethal dose analysis of antimicrobial blue light and photodynamic therapy

Caetano P. Sabino^{a,b,*}, Mark Wainwright^c, Carolina dos Anjos^d, Fábio P. Sellera^d,
Maurício S. Baptista^e, Nilton Lincopan^{b,f}, Martha S. Ribeiro^g

^a BioLambda, Scientific and Commercial LTD, São Paulo, SP, Brazil

^b Department of Clinical Analysis, School of Pharmaceutical Sciences, University of São Paulo, São Paulo, SP, Brazil

^c School of Pharmacy & Biomolecular Sciences, Liverpool John Moores University, Liverpool, UK

^d Department of Internal Medicine, School of Veterinary Medicine and Animal Science, University of São Paulo, São Paulo, SP, Brazil

^e Department of Biochemistry, Institute of Chemistry, University of São Paulo, São Paulo, SP, Brazil

^f Department of Microbiology, Institute for Biomedical Sciences, University of São Paulo, São Paulo, SP, Brazil

^g Center for Lasers and Applications, Nuclear and Energy Research Institute, National Commission for Nuclear Energy, São Paulo, SP, Brazil

ARTICLE INFO

Keywords:

Bacteria
Fungi
Microbial control
Photoantimicrobial
Photoinactivation
Photodynamic antimicrobial chemotherapy
Antimicrobial Photodynamic Therapy

ABSTRACT

Background: Antimicrobial Photodynamic therapy (A-PDT) has been used to treat infections. Currently, microbial inactivation data is reported presenting survival fraction averages and standard errors as discrete points instead of a continuous curve of inactivation kinetics. Standardization of this approach would allow clinical protocols to be introduced globally, instead of the piecemeal situation which currently applies.

Methods: To this end, we used a power-law function to fit inactivation kinetics and directly report values of lethal doses (LD) and a tolerance factor (T) that informs if inactivation rate varies along the irradiation procedure. A deduced formula was also tested to predict LD for any given survival fraction value. We analyzed the photoantimicrobial effect caused by red light activation of methylene blue (MB-APDT) and by blue light (BL) activation of endogenous microbial pigments against 5 clinically relevant pathogens.

Results: Following MB- APDT, *Escherichia coli* and *Staphylococcus aureus* cells become increasingly more tolerant to inactivation along the irradiation process ($T < 1$). *Klebsiella pneumoniae* presents opposite behavior, i.e., more inactivation is observed towards the end of the process ($T > 1$). *P. aeruginosa* and *Candida albicans* present constant inactivation rate ($T \approx 1$). In contrast, all bacterial species presented similar behavior during inactivation caused by BL, i.e., continuously becoming more sensitive to blue light exposure ($T > 1$).

Conclusion: The power-law function successfully fit all experimental data. Our proposed method precisely predicted LD and T values. We expect that these analytical models may contribute to more standardized methods for comparisons of photodynamic inactivation efficiencies.

1. Introduction

Photodynamic therapy (PDT) has been long studied and used to treat localized tumors and infections [1,2]. This light-based technology platform produces cytotoxic molecular species in a space-time controlled manner, i.e., in the absence of light, photosensitizer (PS) or oxygen, photodynamic reactions do not occur. The light-excited PS interacts with molecular oxygen, either by charge (type I reaction) or energy donation (type II reaction), forming a variety of reactive oxygen species (ROS) that can destroy bacteria, parasites, fungi, algae and viral particles [2–7].

The use of PSs thus offers an effective local – not just topical –

approach to infection control, often termed antimicrobial photodynamic therapy (APDT). Importantly, the agency of ROS here means that the conventional resistance status of the microbial target is unimportant. However, in order to provide photosensitization that is fit for purpose, the killing effects of PSs require proper quantification and benchmarking, e.g., the PS concentration and light dose required to destroy a given microbial burden at a certain rate. Standardization of this approach would allow clinical protocols to be introduced globally, instead of the piecemeal situation that currently applies.

According to the Second Law of Photochemistry, for each photon absorbed by a chemical system, only one molecule can be excited and subsequently undergo a photochemical reaction. Based on this

* Corresponding author at: BioLambda, Scientific and Commercial LTD, São Paulo, SP, Brazil.

E-mail address: caetanosabino@gmail.com (C.P. Sabino).

<https://doi.org/10.1016/j.pdpdt.2019.08.022>

Received 15 May 2019; Received in revised form 12 July 2019; Accepted 16 August 2019

Available online 17 August 2019

1572-1000/ © 2019 Elsevier B.V. All rights reserved.

principle, current literature supports photodynamic dosimetry in respect of the number of absorbed photons (*Absorbed Photons/cm³* instead of *J/cm²*) to provide a rather interpretable comparison of PS efficiency [8,9]. It has been proposed that using this method, problematic dosimetry due to variable PS concentration, optical path and excitation wavelength band can be minimized. However, some other problematic situations can be addressed by this method as well. If a filter effect is caused either by high cellular and/or PS concentrations, absorbed photon results may lead to divergent interpretations. Also, Prates et al. [10] have demonstrated that if the number of absorbed photons is kept constant but irradiance varies, the level of microbial inactivation also diverges [10]. These situations suggest the need for a more robust standard method, even though the number of absorbed photons per unit volume can be considered to represent an improvement on merely reporting inactivation as a function of radiant exposure.

Currently, the most accepted form of reporting microbial inactivation data in scientific articles is presenting survival fraction averages and standard errors as discrete points instead of a continuous curve of inactivation kinetics [9,10]. However, analysis of variance over individual points only allows the interpretation of whether those points present statistically significant differences among themselves. Therefore, if one intends to compare the potency of a set of variable antimicrobial photodynamic systems (*i.e.*, different PSs, microbial species, light sources, *etc.*) this analysis may be misguided by local observation of a single point instead of the interpretation of a global kinetics rate. Therefore, this analytical method may lead to false-positive or -negative interpretations in respect to the overall phenomena of microbial inactivation kinetics.

To this end, we report a simple mathematical analysis of continuous bacterial inactivation kinetics curves. We analyzed the photodynamic killing effect caused by red light activation of methylene blue (MB) and by blue light activation of endogenous microbial photosensitive pigments. We expect that this method may assist in developing standardized and more insightful analysis of photoantimicrobial systems.

2. Material and methods

2.1. APDT experiments

In the present study we used the following strains from the American Type Culture Collection (ATCC): *Escherichia coli* (ATCC 25922), *Staphylococcus aureus* (ATCC 25923), *Klebsiella pneumoniae* (ATCC 700603), *Pseudomonas aeruginosa* (ATCC 27853) and *Candida albicans* (ATCC 90028).

Standard APDT susceptibility testing was carried out based on Prates et al. [10]. Inocula were prepared from log-phase overnight cultures. The turbidity of cell suspensions was measured in a spectrophotometer to obtain inocula at McFarland scale 0.5. The scale was calibrated to obtain an optical density of 0.09 at 540 nm and 625 nm resulting in $1-2 \times 10^6$ colony-forming units per milliliter (CFU/mL) of fungi cells, and $1-2 \times 10^8$ CFU/mL of bacterial cells, respectively. Inocula were diluted to a working concentration of $1-2 \times 10^5$ CFU/mL of fungi or $1-2 \times 10^7$ CFU/mL of bacteria.

MB hydrate (purity > 95%, Sigma-Aldrich, USA) was employed as the exogenous PS for this study. Before irradiation, cells were incubated with 100 μ M of MB in phosphate-buffered saline (PBS) for 10 min at room temperature and in the dark, to allow initial uptake. One-mL aliquots were individually placed in clean wells of a 12-well microplate. To avoid cross light exposure, each sample was kept in individual microtubes in the dark during pre-irradiation time and placed in the 12-wells plate only for irradiation.

A red LED probe (660 ± 10 nm, Prototype 1, BioLambda, Brazil) was positioned perpendicularly above each sample, keeping the beam diameter at the bottom of the well at 25 mm (which coincides to a single well diameter from the 12-wells plate). Red light irradiance was kept constant at 100 mW/cm² and radiant exposure levels varied

according to each microbial species sensitivity to MB-APDT as previously determined in pilot experiments.

A blue LED irradiator (415 ± 12 nm, LEDbox, BioLambda, Brazil) was placed below 12-well plates containing 1 mL of each microbial sample. In this case, no exogenous PS was added to the systems. Blue light irradiance was kept constant at 38.2 mW/cm². Radiant exposure levels varied according to each microbial species sensitivity to blue light inactivation as previously determined in pilot experiments.

Immediately after each irradiation process, bacterial suspensions were serially diluted in PBS to give dilutions from 10^{-1} to 10^{-6} times the original concentration. Ten- μ L aliquots of each dilution were streaked onto Mueller-Hinton agar plates, in triplicate, and incubated at 37 °C overnight. A similar procedure was performed for fungi. However, in this case dilutions were between 10^{-1} - 10^{-4} -fold and streaked onto Sabouraud dextrose agar. The colonies were counted and converted into CFU/mL for survival fraction analysis.

2.2. Data analysis

We adapted a power law function to fit inactivation kinetics data in respect to variable radiant exposure levels (equation (1)). Theoretical lethal dose (LD) for any given inactivation rate (*i.e.*, % of bacterial or fungal survival fraction) was calculated according to equation (2). Fitting, residuals and derivatives were calculated using the Prism 7.0 (GraphPad, USA) interface.

$$\log_{10}\left(\frac{N_0}{N}\right) = \left(\frac{\text{Dose}}{\text{LD}_{90}}\right)^T \quad (1)$$

$$\text{LD}_i = \text{LD}_{90} \left(-\log_{10}\left(1 - \frac{i}{100}\right)\right)^{1/T} \quad (2)$$

where:

N_0 = initial microbial burden; N = final microbial burden; *Dose* = light exposure (*e.g.* J, *J/cm²*, time units, *Absorbed Photons/cm³*, *etc.*); LD_{90} = lethal dose for 90% of microbial burden (in light exposure units); T = tolerance factor; i = inactivation percentage (%).

Since data analysis demands some strict procedures to be correctly performed, we organized it into 8 steps as presented in the spreadsheet available in the supplementary material.

Step 1. In Microsoft Excel spreadsheets, we organized the CFU/mL count averages for each experimental replicate according to the light dose delivered. Non-irradiated controls must be identified as 0 units of light dose. The other light doses used can be expressed in Joules, Joules/cm², number of absorbed photons or irradiation time (seconds, minutes or hours).

Step 2. We normalized all survival fraction data in relation to the average CFU/mL counts of non-irradiated controls (*e.g.*, 0 Joules, Joules/cm², number of absorbed photons or irradiation time).

Step 3. Equation (1) only works for survival fraction data converted into Log_{10} units. Therefore, all normalized survival fraction data were individually converted into Log_{10} units before any fitting attempt.

Step 4. We calculated the survival fraction averages and standard deviations from the sets of experimental data of each group. These are the data that must be used in the data analysis software to fit the curve generated by equation (1).

Step 5. We created a new table and graph, organized as XY data configuration, using GraphPad Prism 7 software.

Step 6. After inserting all survival fraction data to Prism 7.0 XY-graph tables, we added equation (1) as an explicit equation for non-linear regressions. This step can be performed through Analyze > XY-analysis > Non-Linear-Regression-(curve fit). A new window will appear with a list of standard equations. Since Prism 7 does not have equation (1) as standard models for fitting data, we added it manually. For such, we clicked on the “+” button to “create a new equation”. On the “Equation” tab, equation type must be set as an explicit equation. In

the “definition” field, we inserted the following formula: $Y = (x/LD_{90})^T$ (T). On the “Rules for Initial Values” tab, we set initial values of LD_{90} and T to be fit as 1. We clicked on “ok” and the new equation was created.

Step 7. If data fitting succeeded, calculated curves will be plotted over data-points in graphs. A table of results will be created on the left panel. This table will present the calculated averages and standard errors for LD_{90} and T.

Step 8. Back in the Microsoft Excel spreadsheet, $LD_{99.9}$ and LD_{100} values were calculated for each dataset using equation (2) in the following formula: $= (LD_{90}) * (-LOG_{10}(1 - (i/100)))^{(1/T)}$ where *i* represents inactivation percentage (%). Due to the inocula used in this study, 100% of inactivation represents $7 \log_{10}$ (99.99999%) for bacteria and $5 \log_{10}$ (99.999%) for yeast.

All experiments were performed in triplicate at 3 different days ($n = 9$), except for MB-APDT against *K. pneumoniae*, which was performed in 4 different days ($n = 12$) due to a pilot study. Survival fraction data were analyzed by Shapiro-Wilk test to confirm normality. Fitted curves were also analyzed using F-test to check if any of the fitted curves are shared by different species. Lethal-dose and T value analysis were compared among species using one-way analysis of variance (ANOVA) with Bonferroni as post-hoc test for multiple comparisons. Results were considered significant if $p < 0.05$.

3. Results and discussion

The Weibull analysis is a well-known and accepted statistical method that uses a power-law function to describe breakdown kinetics of various materials. This analysis assumes that the survival curve is affected by cumulative distributions of damages that leads to lethal effects. Here we assumed that it properly describes effects such as the cumulative oxidative damage imposed by APDT over living cells [11].

Historically, this statistical model has been mostly employed in industries, such as aerospace and automotive, to estimate the reliability on lifespan of mechanical parts [12]. This mathematical function has been used to describe bacterial inactivation kinetics during thermal inactivation or gamma radiation, UV- and blue-light irradiation, free of exogenous PSs [13–16]. However, it has not so far been proposed as a method to standardize APDT sensitivity protocols.

Power-Law fit appears to represent a very good description for APDT inactivation kinetics of our data. Adjusted R^2 values always fluctuated above 0.95 (Table 1). These values represent very good results in relation to general non-linear curve fittings.

The F-test applied over non-linear regressions reported that each species dataset presents a unique inactivation kinetics curve (Fig. 1a-b). This means that even though some inactivation data points may not present statistical differences among species, the entire inactivation kinetics are not the same.

The first derivative of inactivation curves (Fig. 1c-d) further illustrates the variation in inactivation rates. This analysis shows how fast the inactivation occurs during the irradiation procedure. For MB-APDT, *E. coli* and *S. aureus* cells are inactivated rapidly in the beginning of the procedure but slower towards the end of the process. *K. pneumoniae* presents the exact opposite behavior. *P. aeruginosa* and *C. albicans*, however, present almost a constant inactivation rate. On the other hand, all bacterial species presented similar behavior during inactivation caused by blue light alone, i.e., slow initial inactivation but becoming continuously more sensitive to blue light exposure. Conversely,

Table 1
Adjusted R^2 value of each non-linear curve fit.

Species	<i>E. coli</i>	<i>S. aureus</i>	<i>P. aeruginosa</i>	<i>K. pneumoniae</i>	<i>C. albicans</i>
MB-APDT	0.9745	0.9955	0.9939	0.9834	0.9793
Blue Light	0.9691	0.9518	0.9805	0.9526	0.9756

C. albicans presented again almost a constant inactivation rate.

We also submitted inactivation data to double-log transformations in order to confirm data linearization. This is a standard empirical method used to confirm the feasibility of a power-law fit in experimental datasets. As a matter of fact, successful linearization (Fig. 2a-b) further proves the ability to describe photoinactivation kinetics assuming a Power-Law behavior, yet all residual dispersions presented random distributions (Fig. 2c-d).

Non-linear regression results are presented in Fig. 3 as values of the tolerance factor T and lethal doses for 90 percent ($1 \log_{10}$) of inactivation. The tolerance factor T informs the concavity of the inactivation curves; if $T > 1$, cells are initially tolerant to APDT but become increasingly sensitive; if $T < 1$, cells are initially very sensitive, but some persistent cells remain more tolerant to inactivation. Hence, the behavior observed at the inactivation rate curves (Fig. 1c-d) can be indicated by the T values (Fig. 3a-b).

For MB-APDT (Fig. 3a), *S. aureus* and *E. coli* $T < 1$ with no statistically significant difference among themselves; *P. aeruginosa* and *C. albicans* presented T values close to 1, with no statistical difference among themselves; *K. pneumoniae* presented a T value close to 1.5 and was statistically different from all other species treated by MB-APDT. For blue light inactivation, all species presented T values above 1, without any statistically significant differences in between them. These statistical analysis results are presented in tables S1-2 in supplementary material.

Lethal doses for 90% (i.e., $1 \log_{10}$) inactivation with MB-APDT (Fig. 3c) show that *E. coli* and *S. aureus* are the most sensitive and present statistically significant differences to all other species but not among themselves. *P. aeruginosa* presented an intermediate sensitivity to MB-APDT that was significantly different from all other species. *K. pneumoniae* and *C. albicans* are significantly more tolerant to MB-APDT than all other species but not amongst themselves. Even though no statistical differences were observed for T values of blue light inactivation (Fig. 3d), several particularities were reported for lethal dose values. *E. coli* and *S. aureus* are quite sensitive to blue light and present statistically similar behavior. However, *P. aeruginosa* seems to be the most sensitive species tested to blue light, although it did not show statistically significant differences relative to *S. aureus*. Such high sensitivity of *P. aeruginosa* to blue light may be linked to high yield production of pyoverdine, a naturally occurring fluorescent pigment that strongly absorbs 415 nm light and may undergo photodynamic reactions [17,18]. *K. pneumoniae* and *C. albicans* are significantly the most tolerant species to blue light and do not present statistical differences between themselves. These statistical results can be seen in tables S3-4 from supplementary material.

The concept of inactivation rate illustrated by the first derivative of inactivation curves can be specifically quantified by the tolerance factor, presented as T values (Fig. 3a). This is a dimensionless value that indicates the overall inactivation rate behavior. It describes whether cells are more tolerant to inactivation at the beginning of the irradiation process or at the end. Therefore, we can indicate the existence of microbial species with a constitutive tolerance ($T > 1$) that is soon depleted making cells become increasingly sensitive (e.g., MB-APDT for *E. coli* and *S. aureus*); or the presence of adapting or more persistent cells ($T < 1$) that remain harder to kill after a period of irradiation (e.g., blue light for bacteria). Microbial species with T values close to unity may represent an intermediate situation (e.g., *C. albicans* in both situations). The exact tolerance mechanisms responsible for these inactivation kinetics variations may have a multifactorial basis that leads to a constant inactivation rate.

A very useful aspect of using our proposed model is the ability to calculate lethal doses for any given level of survival fraction. Such information allows precise and direct comparisons in between experimental groups and also provides basis for future experimental planning. For example, if one is interested to analyze perspectives of microbial inactivation by APDT or blue light of different experimental groups at

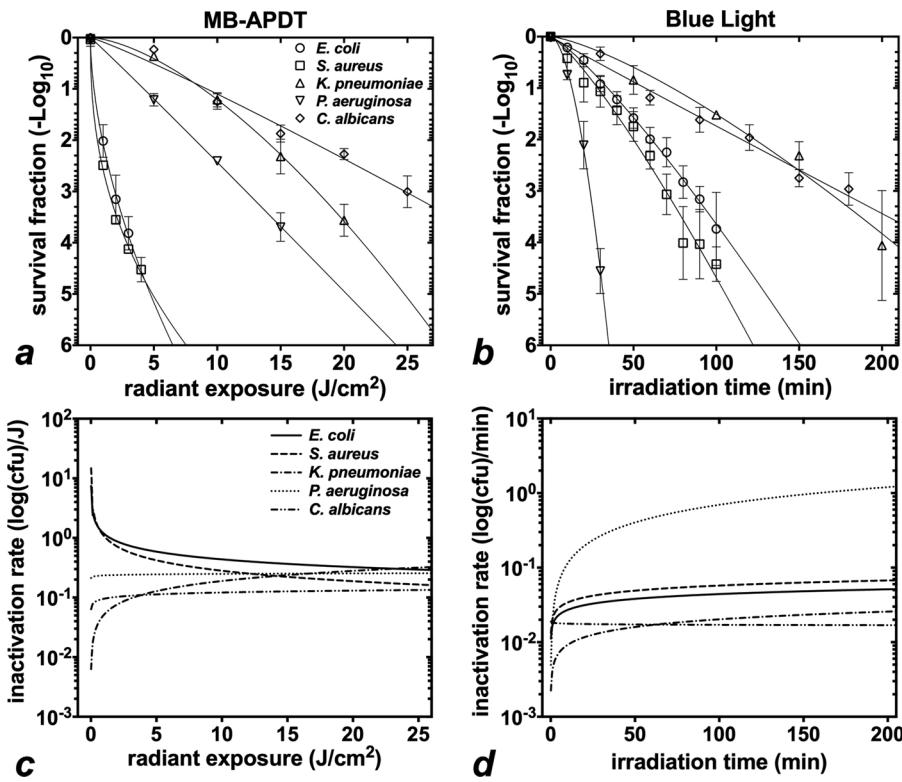


Fig. 1. Inactivation kinetics plots. On the top, survival fraction values are presented for (a) MB-APDT and (b) blue light photoinactivation. Below are the first derivatives (i.e., microbial inactivation rate) of each non-linear regression curves fitted for (c) MB-APDT and (d) blue light photoinactivation. The experimental data from a and b are the log reduction of normalized survival fraction and standard errors.

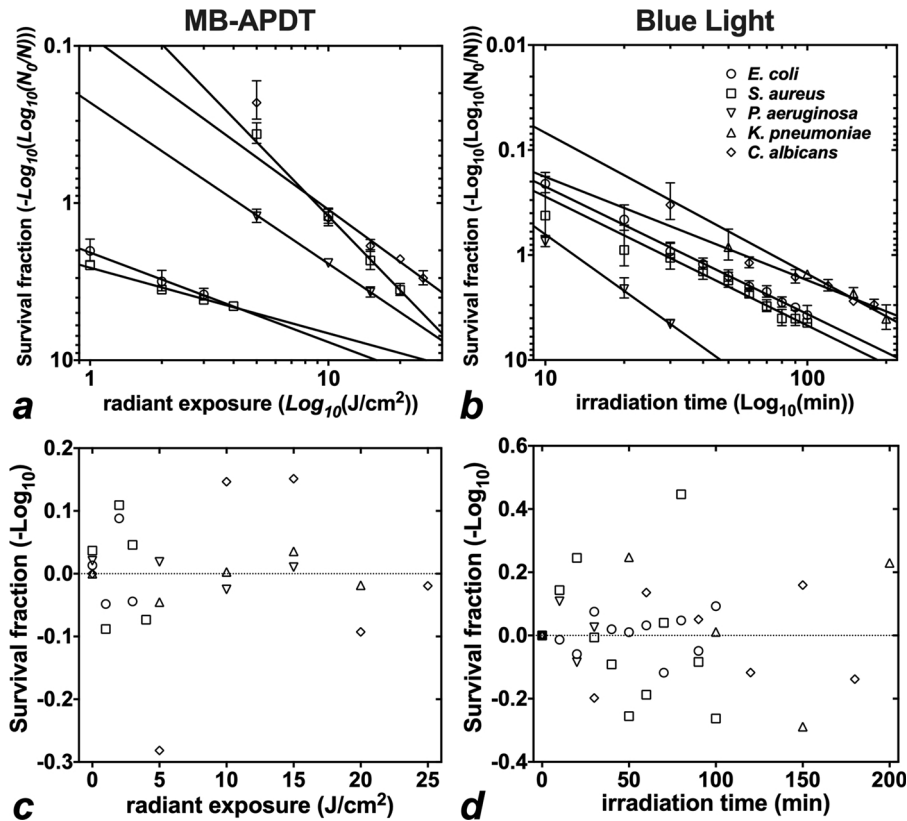


Fig. 2. Linearization of inactivation kinetics data by double-log transformations in a and b confirms the hypothesis of power law function fitting. Residuals of fitted data in c and d presented random distributions around the average, confirming data homogeneity and normality.

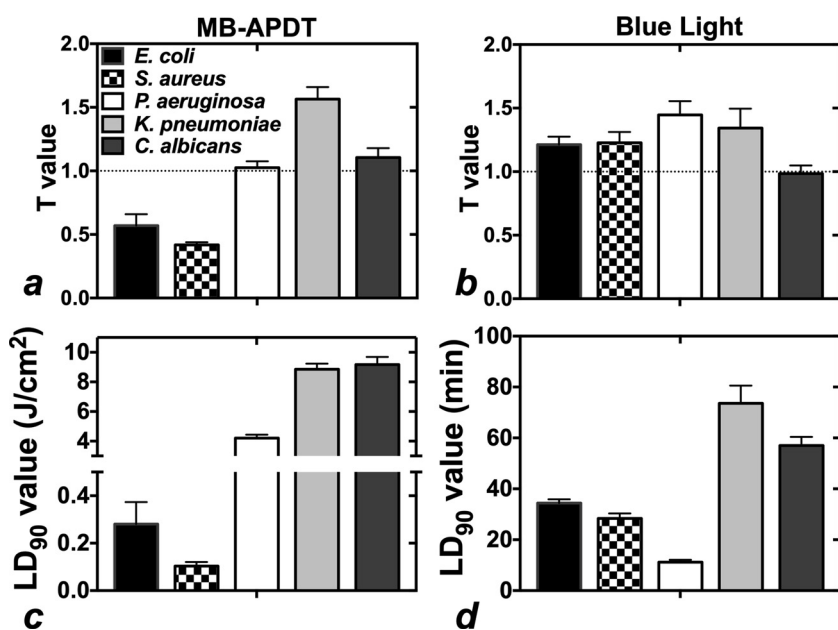


Fig. 3. Non-linear regression parameters of inactivation kinetics obtained for each tested species. On the top, T values are presented for (a) MB-APDT and (b) blue light photoinactivation. Below are the LD₉₀ values calculated for (c) MB-APDT and (d) blue light photoinactivation. The presented values are means of constants and standard errors directly obtained by power law non-linear regressions.

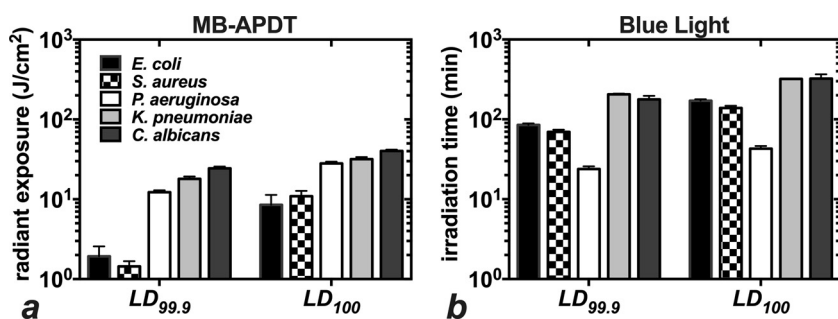


Fig. 4. Lethal dose values calculated for 99.9% ($3\log_{10}$) and 100% ($7\log_{10}$ for bacteria and $5\log_{10}$ for yeast). On the left (a), calculated lethal doses are presented for MB-APDT groups and on the right (b) they are presented for blue light inactivation. The presented values are means and standard errors obtained from data of at least three independent experiments.

the same survival fraction level, this analysis can be used to establish the required light doses. Alternatively, this analysis can also calculate the dose required to achieve complete microbial inactivation (i.e., LD₁₀₀), which is experimentally inviable to measure. In Fig. 4, we used data obtained from equation (1) (e.g., LD₉₀ and T values) to calculate LD_{99.9} and LD₁₀₀ through equation (2). As expected, experimental groups with $T < 1$ presented much greater variations in between LD_{99.9} and LD₁₀₀ than groups with $T > 1$. The statistical results respective to data from Fig. 3 are presented in tables S5-6 from supplementary material.

For experimental verification of our proposed model, we compared photodynamic inactivation kinetics of MB-APDT and blue light using diverse species of clinically relevant pathogens. MB currently is the most broadly PS used in APDT studies while blue light inactivation is a promising antimicrobial platform using novel high-powered blue LEDs. These surrogates represent very different approaches to light-mediated microbial control and, yet, Eq. (1) successfully fit all tested data. We also showed that doses can be reported in time or energy units with no detriment of the analysis output. Thus, we expect that other PS classes should also be suitable for such analysis, and that this approach will allow the development of standardized protocols for photodynamic antimicrobial therapies. This way, future studies that choose to use this model could report quantitative data regarding LD₉₀ and T values in order to allow comparative analysis between different PS, light sources, irradiances, etc. We hope to motivate further studies to employ this method also for experiments regarding *in vitro* biofilms and *in vivo* infections.

4. Conclusion

We reported a mathematical model to fit and describe photoinactivation kinetics in interpretative and quantitative terms. A power-law function successfully fit all data from experiments performed with MB-APDT and blue light alone. A deduced formula could also be used to precisely predict lethal doses for any given survival fraction value. We truly expect that these analytical methods may contribute to a more standardized protocol for comparisons of photodynamic inactivation efficiency.

Declaration of Competing Interest

C. P. Sabino is an associate at BioLambda but declares to only have scientific interest on this study. There are no further conflicts of interest to be declared.

Acknowledgments

We gratefully thank the Brazilian fostering agency FAPESP (grants 2013/07937-8, < GN1 > 2016/08593-9, < GN1 > 2016/25095-2, < GN1 > 2017/22406-0), CNPq (grants < GN2 > 465763/2014-6, < GN2 > 141901/2016-0, < GN2 > 312249/2017-9) < /GN2 > < /GN2 > < /GN1 > < /GN1 > < /GN1 > and technical support offered by the start-up company BioLambda.

Appendix A. Supplementary data

Supplementary material related to this article can be found, in the

online version, at doi:<https://doi.org/10.1016/j.pdpdt.2019.08.022>.

References

- [1] P. Agostinis, K. Berg, K.A. Cengel, T.H. Foster, A.W. Girotti, S.O. Gollnick, et al., Photodynamic therapy of cancer: an update, *CA Cancer J. Clin.* 61 (4) (2011) 250–281.
- [2] M. Wainwright, Photodynamic antimicrobial chemotherapy (PACT), *J. Antimicrob. Chemother.* 42 (1) (1998) 13–28.
- [3] T. Maisch, S. Hackbarth, J. Regensburger, A. Felgentrager, W. Baumler, M. Landthaler, et al., Photodynamic inactivation of multi-resistant bacteria (PIB) - a new approach to treat superficial infections in the 21st century, *J. Dermatol. Ges.* 9 (5) (2011) 360–366.
- [4] T. Dai, Y.Y. Huang, M.R. Hamblin, Photodynamic therapy for localized infections—state of the art, *Photodiagnosis Photodyn. Ther.* 6 (3–4) (2009) 170–188.
- [5] J.P. Lyon, L.M. Moreira, P.C. de Moraes, F.V. dos Santos, M.A. de Resende, Photodynamic therapy for pathogenic fungi, *Mycoses* 54 (5) (2011) e265–71.
- [6] R. Schmidt, Photosensitized generation of singlet oxygen, *Photochem. Photobiol.* 82 (5) (2007) 1161–1177.
- [7] F.P. Sellera, C.P. Sabino, M.S. Ribeiro, R.G. Gargano, N.R. Benites, P.A. Melville, et al., *In vitro* photoinactivation of bovine mastitis related pathogens, *Photodiagnosis Photodyn. Ther.* 13 (2016) 276–281.
- [8] B.C. Wilson, M.S. Patterson, L. Lilje, Implicit and explicit dosimetry in photodynamic therapy: a New paradigm, *Lasers Med. Sci.* 12 (3) (1997) 182–199.
- [9] F. Cieplik, A. Pummer, J. Regensburger, K.A. Hiller, A. Spath, L. Tabenski, et al., The impact of absorbed photons on antimicrobial photodynamic efficacy, *Front. Microbiol.* 6 (2015) 706.
- [10] R.A. Prates, E.G. Silva, A.M. Yamada, L.C. Suzuki, C.R. Paula, M.S. Ribeiro, Light parameters influence cell viability in antifungal photodynamic therapy in a fluence and rate fluence-dependent manner, *Laser Phys.* 19 (5) (2009) 1038–1044.
- [11] W. Weibull, A statistical distribution function of wide applicability, *J. Appl. Mech.* 18 (3) (1951) 293–297.
- [12] G.W. Weibull, Citation classic - a statistical distribution function of wide applicability, *Cc/Eng Tech. Appl. Sci.* (10) (1981) 18.
- [13] D.L. Holcomb, M.A. Smith, G.O. Ware, Y.C. Hung, R.E. Brackett, M.P. Doyle, Comparison of six dose-response models for use with food-borne pathogens, *Risk Anal.* 19 (6) (1999) 1091–1100.
- [14] X. Hu, P. Mallikarjunan, J. Koo, L.S. Andrews, M.L. Jahncke, Comparison of kinetic models to describe high pressure and gamma irradiation used to inactivate *Vibrio vulnificus* and *Vibrio parahaemolyticus* prepared in buffer solution and in whole oysters, *J. Food Prot.* 68 (2) (2005) 292–295.
- [15] K. McKenzie, M. Maclean, I.V. Timoshkin, E. Endarko, S.J. MacGregor, J.G. Anderson, Photoinactivation of bacteria attached to glass and acrylic surfaces by 405 nm light: potential application for biofilm decontamination, *Photochem. Photobiol.* 89 (4) (2013) 927–935.
- [16] H. Bozkurt, D.H. D'Souza, P.M. Davidson, Determination of thermal inactivation kinetics of hepatitis A virus in blue mussel (*Mytilus edulis*) homogenate, *Appl. Environ. Microbiol.* 80 (10) (2014) 3191–3197.
- [17] R.P. Elliott, Some properties of pyoverdine, the water-soluble fluorescent pigment of the pseudomonads, *Appl. Microbiol.* 6 (4) (1958) 241–246.
- [18] C. Propst, L. Lubin, Light-mediated changes in pigmentation of *Pseudomonas aeruginosa* cultures, *J. Gen. Microbiol.* 113 (2) (1979) 261–266.